

SECURITY INFORMATION
CONFIDENTIAL

SECRET

243
2-17-58

AD No. 25716
ACTIVE FILE COPY

WIDE APERTURE DISTRIBUTION OF ABI SYSTEMS WITH OPTICAL SUPERPOSITION (WADABIS)

This document has been reviewed in accordance with
OPNAVINST 5510.17, paragraph 5. The security
classification assigned hereto is correct.

Dated 7/24/58

Robert H. Miller
By direction of
Chief of Naval Research (Code 422)

N6-04-07115

Project No. ONR 076-161

TECHNICAL REPORT NO. 19



ELECTRICAL ENGINEERING RESEARCH LABORATORY
ENGINEERING EXPERIMENT STATION
UNIVERSITY OF ILLINOIS
URBANA, ILLINOIS

54AA-13023

WIDE APERTURE DISTRIBUTION OF ABI SYSTEMS
WITH OPTICAL SUPERPOSITION (WADABIS)
N6-ori-7115 ONR Project No. 076-161

Date:
January 1954

Prepared by:

H. D. Webb

R. L. Sydnor

Approved by:

Harold D. Webb

H. D. Webb

Associate Professor

NOTICE

This document contains information affecting the national defense of the United States within the meaning of the Espionage Laws, Title 18, USC, Sections 793 and 794. The transmission or the revelation of its contents in any manner to an unauthorized person is prohibited by law.

E. C. Jordan
E. C. Jordan
Professor

RADIO DIRECTION FINDING SECTION
ELECTRICAL ENGINEERING RESEARCH LABORATORY
ENGINEERING EXPERIMENT STATION
UNIVERSITY OF ILLINOIS
URBANA, ILLINOIS

CONFIDENTIAL

FOREWORD

It has been fairly well established that accurate and instantaneous direction finding on multi-path transmissions (such as normally occur in the high-frequency band) requires the use of wide-aperture systems; that is, systems which are large in wavelengths. Essentially what is required is a sampling of the field at a number of points in an area of several square wavelengths. This sampling may be done with a wide-aperture system of which several have been proposed, or alternatively, by a distribution of narrow-aperture systems. The WADONAS (Wide Aperture Distribution of Narrow Aperture Systems) described in Technical Report #10 is an example of the latter method. The WADONAS makes use of a superposition of elliptical displays such as are normally obtained with the matched-channel (Watson-Watt) type of radio direction finder. The superposition of ellipses results in a polygonal figure from which the directions of arrival of the component waves can be determined. The possibility of an actual field trial of such a system is rather remote owing to the fact that the Navy does not presently use the elliptical display, but instead uses the propeller-shaped pattern obtained from a rotating-goniometer type system. Superposition of these propeller-shaped patterns yields little useful information. However, because these latter patterns before rectification contain the same information available from the ellipses, it appears that it should be possible to transform one display into the other. Such a transformation would provide the possibility of utilizing present group d-f installations to give a WADONAS type display.

In this report the authors have explored methods of performing this transformation of displays and have built a "bread-board" model of one particular method to verify the correctness of the principle and to ascertain some of the practical limitations. Although much more developmental work would be required to produce a practical working model, the research has been carried far enough to demonstrate the basic soundness of the idea.

E. C. Jordan

ABSTRACT

It has been shown previously that outputs from a space distribution of Watson-Watt, or twin-channel, RDF systems may be combined optically to produce a display that could be used to give accurate bearings on signals of short duration. In this report a method is described for transforming the ABI (Automatic Bearing Indicator) displays to a form suitable for optical superposition.

The signals from the N-S and E-W pairs of antennas are labeled in quadrature by modulating them with the goniometer rotation rate before the signals are fed into the ABI receiver. These signals are preserved at the IF output of the ABI receiver, and contain all of the information of a Watson-Watt system. A bread-board system is described wherein the labeled signals are separated by quadrature detection and fed into separate channels where there is a frequency conversion to twice the goniometer rate. Band pass amplifiers centered at this low frequency are used in combination with suitable filters for eliminating undesired components. The outputs from these amplifiers are fed to the orthogonal plates of a CRT to obtain the Watson-Watt type display. Photographs showing the transformed results are presented.

A discussion of some of the practical limitations is given, as are some alternate methods of accomplishing the same sort of results. The quadrature modulation may be done by electronic means at either high or low audio frequencies, provided that the prescribed precautions are taken.

TABLE OF CONTENTS

	<i>Page</i>
Foreword	ii
Abstract	iii
List of Symbols	1
1. Introduction	2
2. Methods of Transforming the ABI Intermediate Frequency Output to the Watson-Watt-Type of Display	8
3. Detailed Description of Bearing Transformation System	14
4. Experimental Results	24
5. Limitations and Alternate Methods of Operation	28
6. Conclusions	30
7. Bibliography	31
Appendix A - Equality of Ellipsing in the Watson-Watt and Blurring in the Modified ABI	32
Appendix B - Development of the Display Equation for the Transformation Method Using Square-Law Balanced Modulators	36
Appendix C - Development of the Display Equation for the Transformation Method Using Linear Mixers	38
Appendix D - The Effect of Modulation on the Transformation System	40

ILLUSTRATIONS

Number		Page
1	WADONAS Displays for Two Arriving Signal Components	3
2	Watson-Watt Displays for One and Two Arriving Signal Components	4
3	ABI Displays for One and Two Arriving Signal Components	6
4	"Figure-Eight" Patterns Obtained by Displaying the ABI IF Output	7
5	Block Diagram of Bearing Transformation System that Gives Only Straight Line Displays	10
6	Superposition of Straight Line ABI Transformation	11
7	Block Diagram of ABI to Watson-Watt Bearing Transformation System	13
8	Circuit Diagram of the Goniometer Driver	15
9	Circuit Diagram of the Linear Mixer	16
10	Circuit Diagram of the Amplifier and Low-Pass Filter	17
11	Circuit Diagram of the Band-Pass Amplifier	19
12	Circuit Diagram of the Band-Block Filter	20
13	Frequency Response Curves of Band-Pass Amplifier and Band-Block Filter	21
14	Circuit Diagram of the Deflection Amplifier	22
15	ABI "Figure-Eight" and Transformed Displays for Signals on one Frequency	25
16	ABI "Figure-Eight" and Transformed Displays for Signals on Two Frequencies	26
17	Relationship Between ABI and Watson-Watt Displays	34

LIST OF SYMOBLS

α = the angle of arrival of strongest signal component

$\frac{\theta}{2\pi}$ = the goniometer rotation rate in rps

p = an integer representing one of the interfering signal components

N = the total number of interfering signal components

H_p = the ratio of the amplitude of the p^{th} signal component to the amplitude of the strongest signal component

ϕ_p = the phase angle between the p^{th} signal component and the strongest signal component,

β_p = the angle between the direction of arrival of the p^{th} signal component and the direction of arrival of major component

$\frac{\omega}{2\pi}$ = the intermediate frequency of either the ABI or Watson-Watt receiver

q = an integer representing one of the modulation frequencies

s = the total number of modulation frequencies

m_q = the ratio of the magnitude of the q^{th} modulation frequency component to the magnitude of the carrier, i.e. the modulation index of the q^{th} component,

$\frac{\sigma_q}{2\pi}$ = the q^{th} modulation frequency in cps

$\frac{\rho}{2\pi}$ = an arbitrary frequency in cps

1. INTRODUCTION

Technical Report No. 10 on this contract² described a method of optically superimposing the outputs from several narrow aperture Watson-Watt, or twin-channel, RDF systems arranged in an array. The composite display on a multigun oscilloscope is a polygon having n -pairs of parallel sides, where n represents the number of arriving signal components. The direction of arrival and relative strength of each of the signal components may be determined from the display. From the display the bearing of the strongest signal component or the average indicated bearing may be determined. Figure 1 shows the type of display that is obtained from such a superposition.

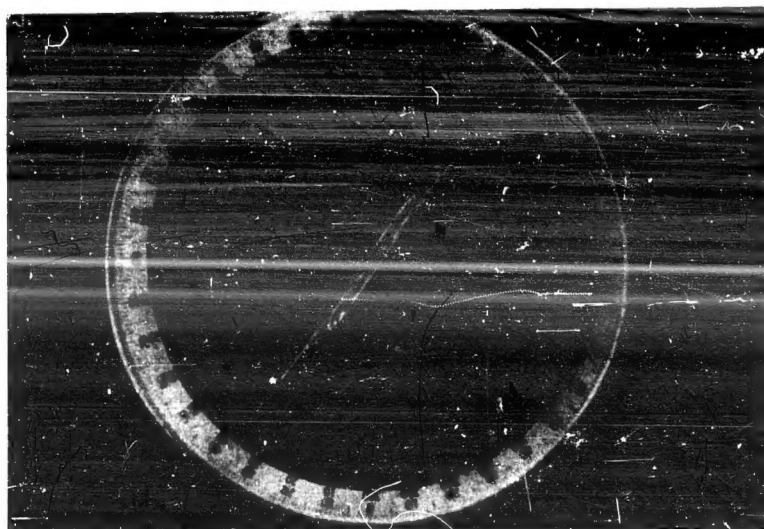
The display from each Watson-Watt system is either a straight line or an ellipse. For each system position in the array of systems the aspect of the elliptical indication is, in general, different from that at any other position, and, with properly adjusted gains, the composite of all possible aspects of the elliptical indication gives the polygon display. With only a few systems in the array, say 5 to 7, the envelope of the polygon may be determined. Pictures of Watson-Watt displays for one and two arriving signal components are shown in Fig. 2.

The composite display from the system just described may be obtained from Watson-Watt displays because the Watson-Watt displays are either straight lines or ellipses for signals with all components on the same frequency. The composite display, referred to in other reports as the WADONAS display, has a definite advantage in permitting bearing data on signals of very short duration.

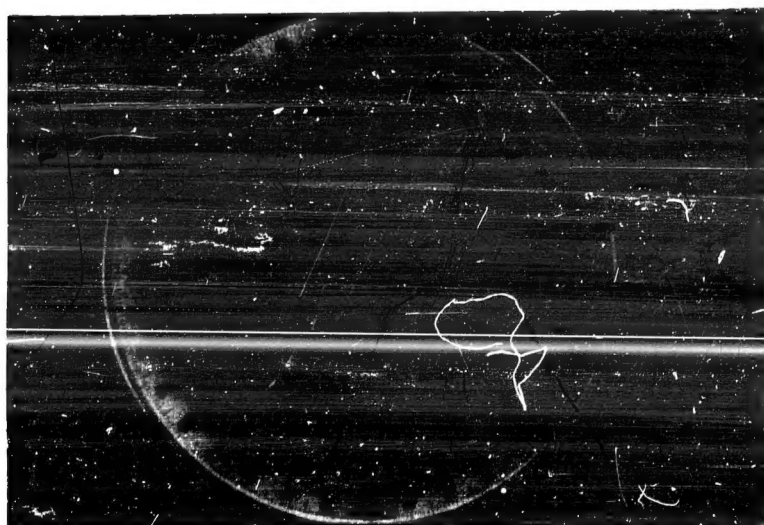
The ABI, or Automatic Bearing Indicator, display is a "propeller-shaped" display. When there is only one signal present the display is sharply defined, with a deep null along a line at right angles to the indicated bearing. When two signal components on one frequency are present the propeller-shaped pattern becomes blurred. When these components are slightly different in frequency the phase angle between them varies, and the display becomes a cusped figure which is somewhat difficult to interpret, especially if modulation is present. This figure represents the envelope for a composite display made up by superimposing the displays from a distribution of ABI systems. If more than two signal components are present the envelope for the composite display



a. Angle of separation of components is 30° .
Relative amplitudes of components is 0.4.

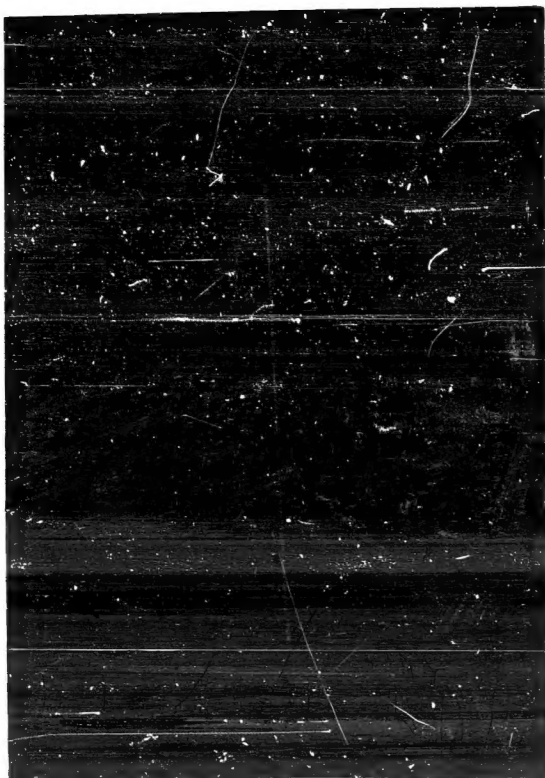


b. Angle of separation is 15° .
Relative amplitude is 0.4.



c. Angle of separation is 10° .
Relative amplitude is 1.

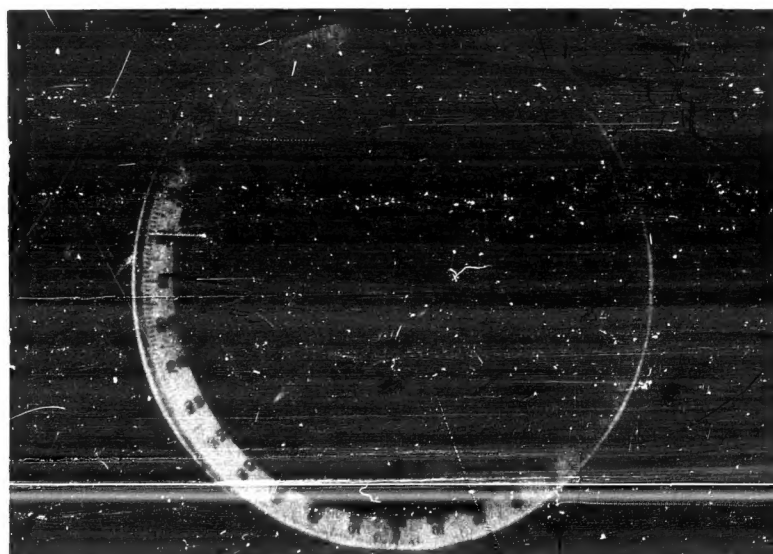
FIGURE 1 WADONAS DISPLAYS FOR TWO ARRIVING SIGNAL COMPONENTS



a. A single signal component



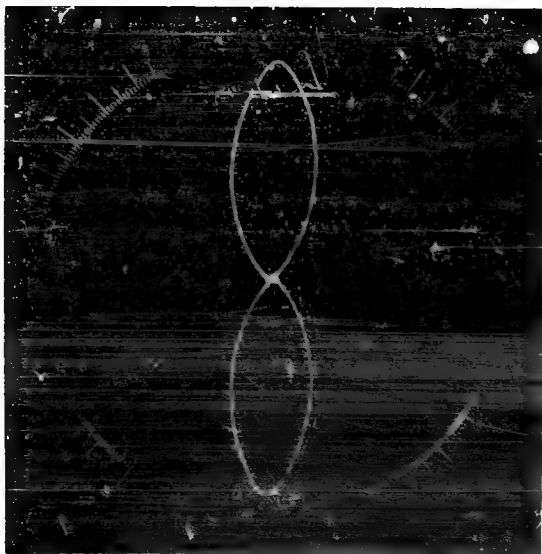
b. Two signal components at the same frequency



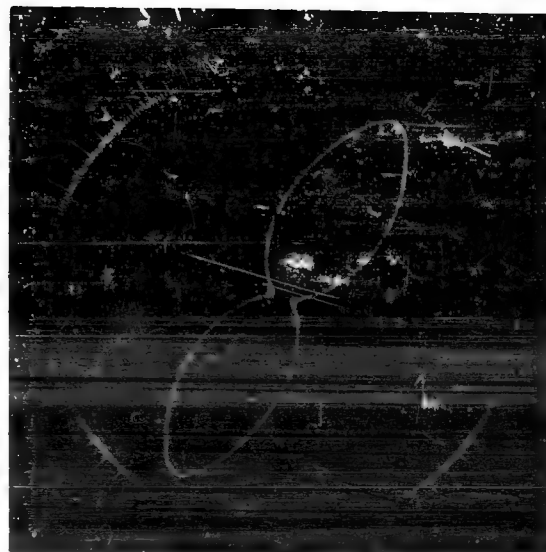
c. Two signal components at different frequencies

FIGURE 2 WATSON-WATT DISPLAYS FOR ONE AND TWO ARRIVING SIGNAL COMPONENTS

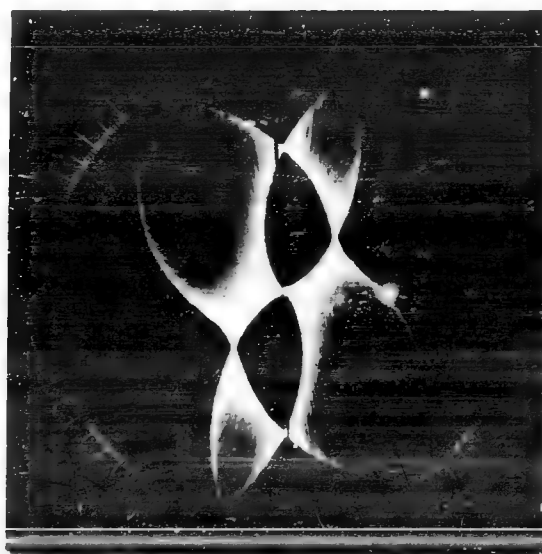
is even more complicated and confusing. Pictures of ABI displays for one and two signal components are shown in Fig. 3. At the output of the ABI intermediate frequency amplifier, the display would give a "figure-eight" pattern, such as those indicated in Fig. 4. The ABI pattern is obtained by subtracting the "figure-eight" pattern envelope from a circle. This "figure-eight" signal, before rectification, contains all of the information put into the receiver from the antennas except those portions which have been eliminated by the filter action of the tuned circuits in the receiver. There is a one-to-one correspondence between the "blur" of the "figure-eight" pattern of the ABI at IF and the ellipsing of the Watson-Watt pattern. A development illustrating this correspondence is given in Appendix A. This fact indicates that it should be possible to operate on the figure-eight pattern at IF in some manner and obtain the elliptical, or Watson-Watt-type, indication.



a. A single signal component

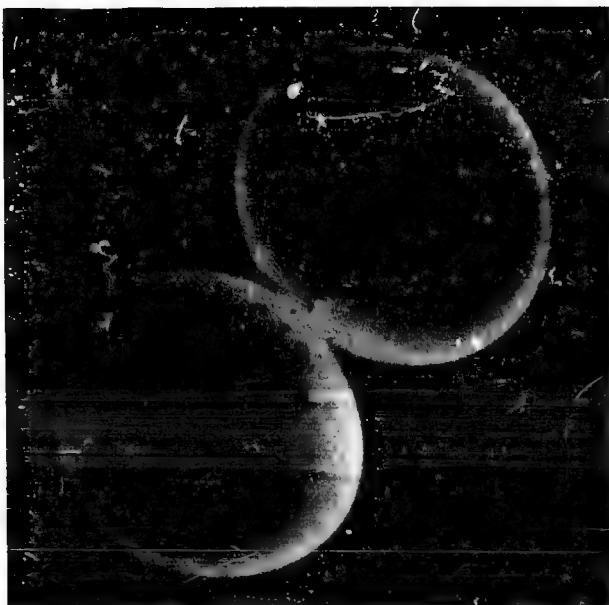


b. Two signal components at the same frequency

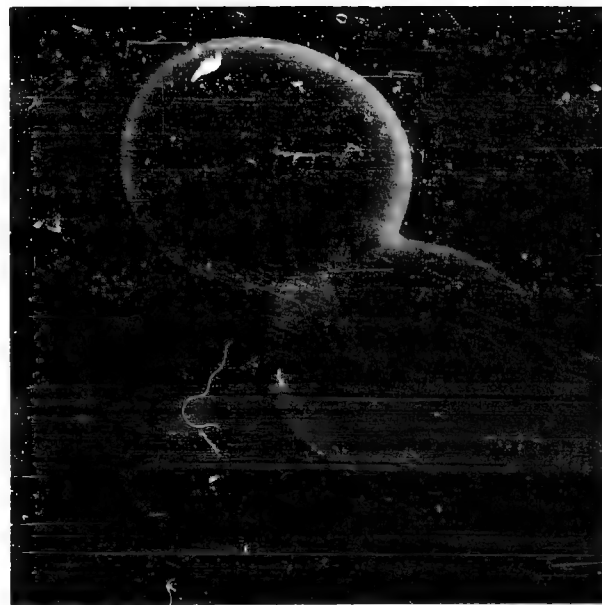


c. Two signal components at different frequencies

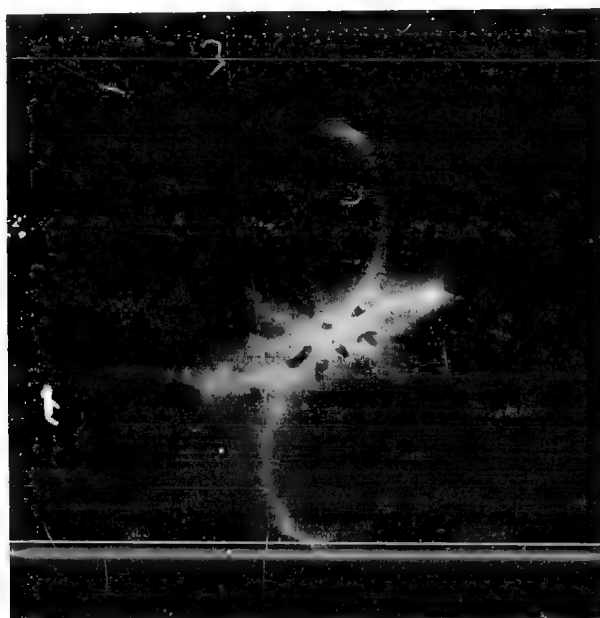
FIGURE 3 ABI DISPLAYS FOR ONE AND TWO ARRIVING SIGNAL COMPONENTS



a. A single signal component



b. Two signal components at the same frequency



c. Two signal components at different frequencies

FIGURE 4 FIGURE-EIGHT PATTERNS OBTAINED BY DISPLAYING THE ABI IF OUTPUT

2. METHODS OF TRANSFORMING THE ABI INTERMEDIATE-FREQUENCY OUTPUT TO THE WATSON-WATT-TYPE OF DISPLAY

The intermediate frequency output display of the ABI receiver:

$$E = A \cos \omega t \cos (\alpha - \theta t) e^{j\theta t} + A \sum_{p=0}^N H_p \cos (\omega t + \phi_p) \cos (\alpha + \beta_p - \theta t) e^{j\theta t} \quad (1)$$

is to be transformed in such a manner that a display of the Watson-Watt type:

$$Z = B \cos \omega t e^{j\alpha} + B \sum_{p=0}^N H_p \cos (\omega t + \theta_p) e^{j\alpha + \beta_p} \quad (2)$$

is obtained.

The ABI receiver may be regarded as a labeling device which labels the signals from the two antenna pairs and adds them before amplification and detection. This process corresponds to a synchronous modulation process in which the two signals are modulated with quadrature components of another signal, in this case the goniometer rotation rate, which is $\theta/2\pi$ revolutions per second.

A means of separating the two components of the intermediate-frequency output of the ABI receiver is required, or, in other words, a means of synchronous detection. It appears that the most straightforward means of doing this is to modulate the output with two orthogonal signals at the same frequency as the receiver goniometer rotation rate. This can be accomplished by applying the intermediate-frequency output voltage of the ABI receiver to the search coil of a second goniometer which is mechanically coupled to the original receiver goniometer and which has the same displacement angle (θt). Then the voltage across the orthogonal stators of the goniometer are the original IF voltage of the ABI receiver, modulated by $E_m \cos \theta t$ and $E_m \sin \theta t$ respectively.

These two voltages contain the required terms along with undesired terms. Several means of eliminating the undesired terms are possible.

If each of these voltages is applied to separate square-law balanced modulators, where the frequency of the modulating voltage differs from

the intermediate-frequency of the ABI receiver by any constant phase angle, γ , and all AC terms are eliminated by filters, two DC voltages proportional to $\sin \alpha$ and $\cos \alpha$, respectively, would be obtained. Modulating with a signal of some arbitrary frequency (probably low-audio frequency for simplicity) and applying the two voltages thus obtained to the two pairs of deflection plates of a cathode-ray oscilloscope results in a display which may be represented by:

$$Z = K \sin pt \left[\cos \gamma e^{j\alpha} + \sum_{p=0}^N H_p \cos (\gamma - \phi_p) e^{j(\alpha + \beta_p)} \right] \quad (3)$$

The development of this expression is given in Appendix B. A block diagram of a system of this type is shown in Fig. 5.

This is not exactly the same form as the Watson-Watt display represented by Eq. (2) since no ellipsing would occur for two signal components of the same frequency. For purposes of optical superposition, as in the WADABI, straight lines would work, but in order to determine an envelope, many more straight lines than ellipses would be required.

The display for this system would be as shown in Fig. 6a, where the position of the straight line may take any position from \overline{aod} to \overline{boc} , depending on the relative phase of the two signal components. If the signals were not at exactly the same frequency, but only slightly different so that the filters would not separate them, all possible positions of the straight line would give the parallelogram envelope shown in dotted lines. The optical superposition of displays of this type would determine the parallelogram envelope if enough individual displays were used. The parallelogram envelope is shown in Fig. 6b.

For three signal components the straight line would eventually describe a display such as is shown in Fig. 6c when the components vary slowly in phase. Similarly for any number of signal components the envelope will be a polygon having N pairs of parallel sides. This polygon is the same as would be indicated by the Watson-Watt display and may be interpreted in the same manner. For purposes of optical superposition, this transformation system is satisfactory, but has the disadvantage that many small aperture systems would be required in order to determine the polygon envelope.

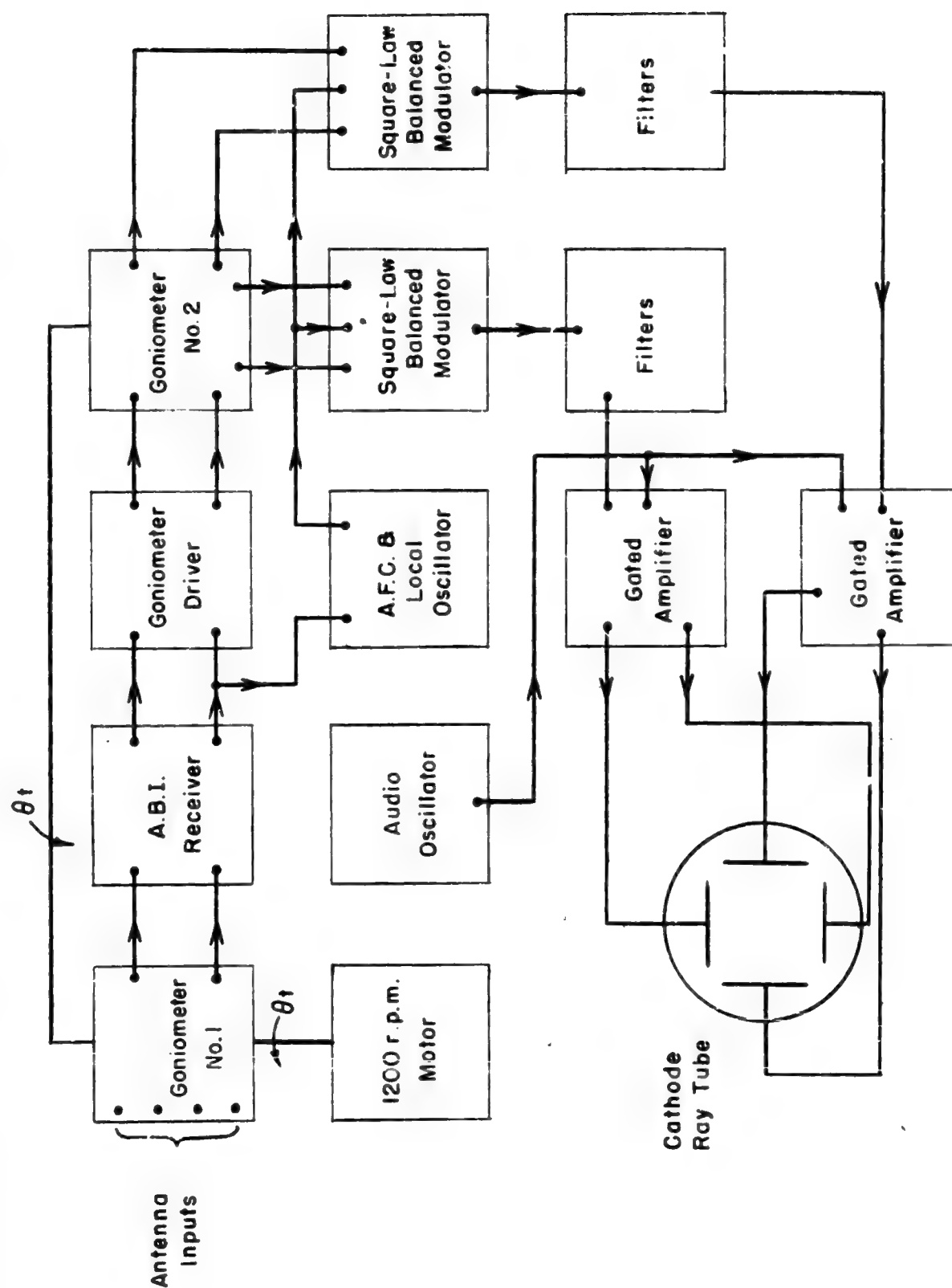


FIGURE 5 BLOCK DIAGRAM OF BEARING TRANSFORMATION SYSTEM THAT GIVES ONLY STRAIGHT LINE DISPLAYS

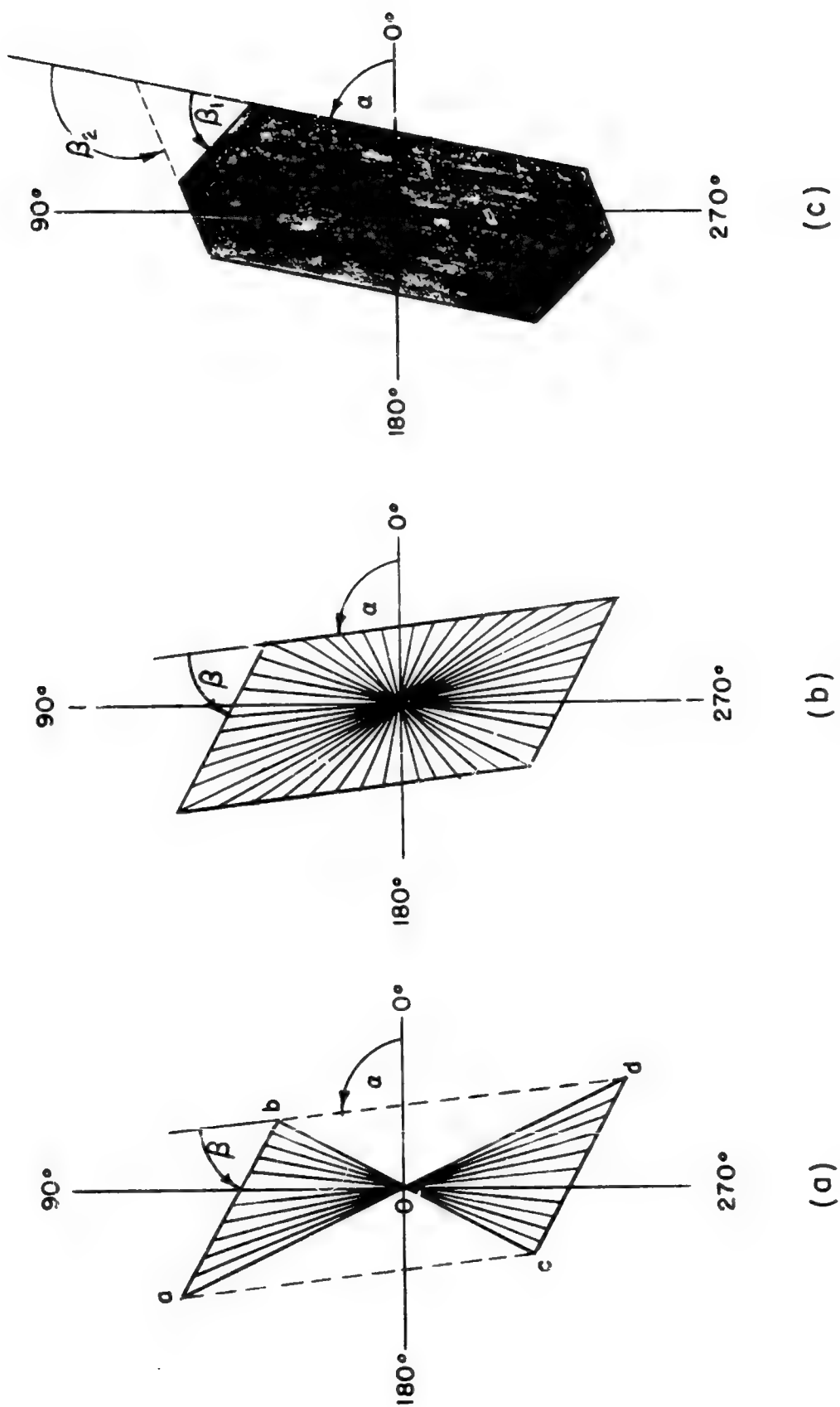


FIGURE 6 SUPERPOSITION OF STRAIGHT LINE ABI TRANSFORMATION

An alternate method of transforming the IF output of the ABI to the Watson-Watt-type of display is as follows:

- A. modulate the IF output with a second goniometer as above,
- B. use some sort of linear multiplier to multiply the voltages obtained in (A) by $E_n \cos (\omega t + 2\theta t)$,
- C. filter out all terms from (B) which are not of the frequency $\frac{2\theta}{2\pi}$
- D. apply the resulting voltages to the orthogonal plates of a cathode-ray oscilloscope.

The display for this system may be represented by:

$$Z = M \left[\cos 2\theta t e^{j\alpha} + \sum_{p=0}^N H_p \cos (2\theta t - \phi_p) e^{j(\alpha + \beta_p)} \right], \quad (4)$$

which is the same as the Watson-Watt display indicated by Eq. (2), except for a substitution of $2\theta t$ for ωt . The development for this result is given in Appendix C.

The latter is the system that was developed. It is shown by block diagram in Fig. 7.

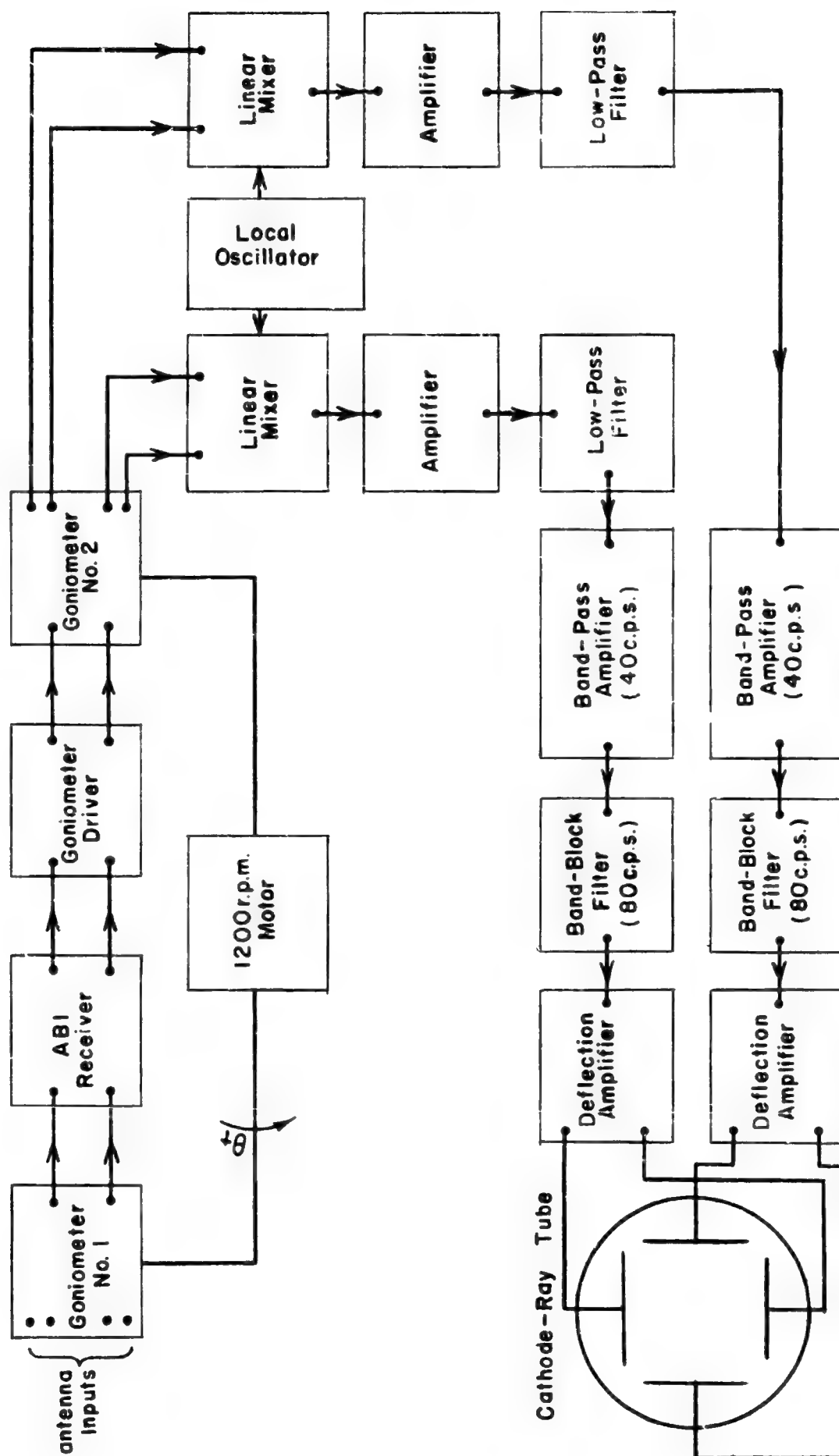


FIGURE 7 BLOCK DIAGRAM OF ABI TO WATSON-WATT BEARING TRANSFORMATION SYSTEM

3. DETAILED DESCRIPTION OF BEARING TRANSFORMATION SYSTEM

3.1 Goniometer Driver

A suitable method of driving the goniometer was found necessary because of its extremely low impedance and variability of impedance with rotation angle.

The low impedance driver needed suggested cathode follower type amplifiers. The output power needed was relatively large since voltages on the order of one volt were required. For these reasons and because of the relative independence of gain of cathode followers with variations in tube parameters, six type 12AU7 dual-triodes connected in parallel were used on each side of a push-pull amplifier. In order to minimize distortion caused by driving the grids of this power amplifier positive, cathode followers were used to drive the power stages. The circuit diagram for the goniometer driver is shown in Fig. 8.

3.2 Linear Mixer

The requirement that the output of a mixer be of the form:

$$E_{out} = C_1 E_a + C_2 E_b + C_3 E_a E_b, \quad (5)$$

with very low amplitude higher order terms, places a very severe limitation on circuitry and tube types.

After testing all of the available miniature pentagrid converters, a pair of type 6BA7 tubes were used with the circuit shown in Fig. 9. While these were the best of all tubes of the miniature type that were tested, higher order terms were not negligible and the constant C_3 in the above equation was very small. Testing the available octal type tubes resulted in the use of type 6SA7 tubes since, of all tubes tested, this type was the best suited for this purpose.

3.3 Amplifier and Low-Pass Filter

Because of the low level of the desired components and fairly high level of undesired components in the output of the mixers, a low-pass filter was found necessary to prevent overdriving the succeeding stages with undesired components. The amplifiers and filters are conventional circuits and need no further mention. The circuit diagram is given in Fig. 10.

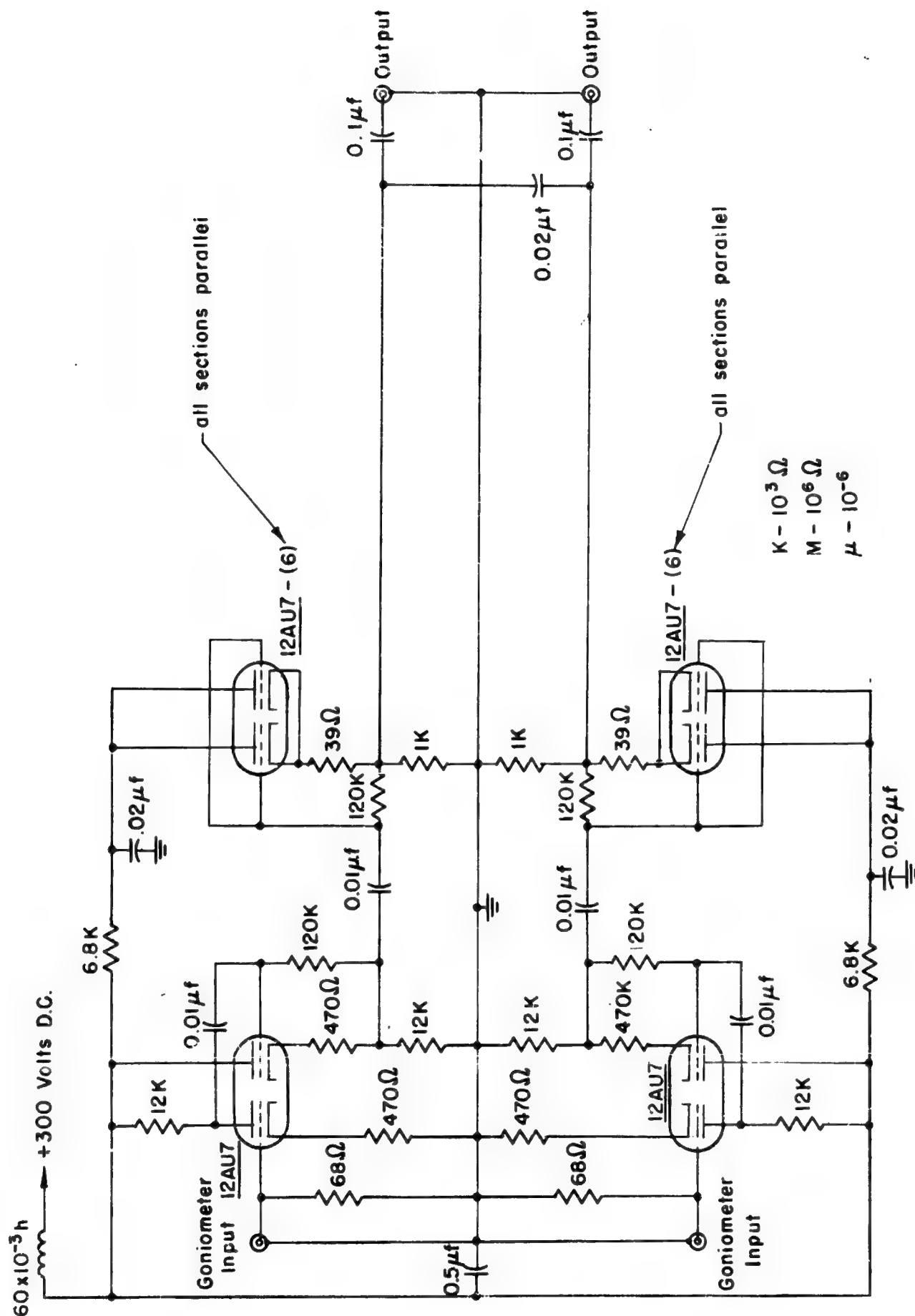


FIGURE 8 CIRCUIT DIAGRAM OF THE GONIOMETER DRIVER

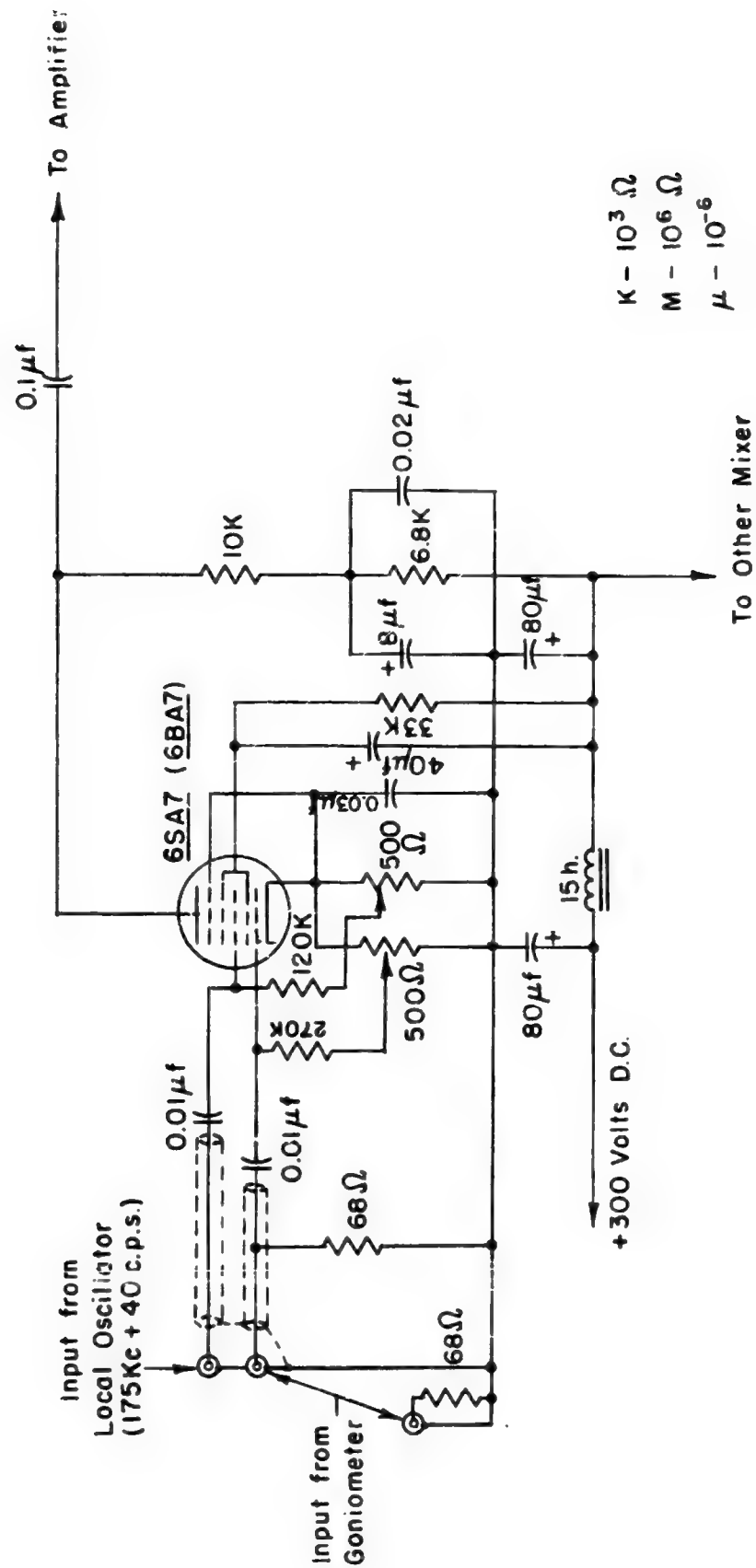
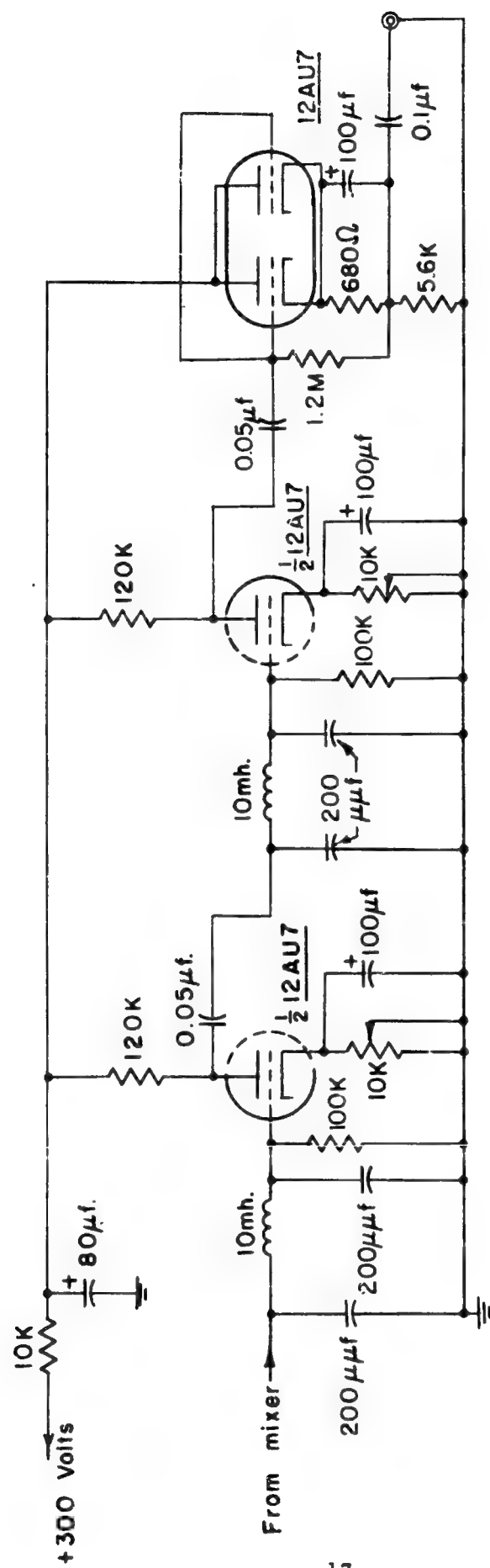


FIGURE 9 CIRCUIT DIAGRAM OF THE LINEAR MIXER



$K - 10^3 \Omega$
 $M - 10^6 \Omega$
 $m - 10^{-3}$
 $\mu - 10^{-6}$
 $\mu\mu - 10^{-12}$

FIGURE 10 CIRCUIT DIAGRAM OF THE AMPLIFIER AND LOW-PASS FILTER

3.4 Band-Pass Amplifier

The band-pass amplifier consists of two stages of feedback amplifiers with twin-T β -networks.⁵ The circuit diagram is shown in Fig. 11. The components selected for the β -networks were matched to within one-percent and were of high quality to insure the stability of these amplifiers. The constant-current pentodes insured stable operation under a wide range of input impedances of the β -network. Curves of frequency response are shown in Fig. 13a and b. The time variation in frequency, gain, and band-width were such that, after the two channels were once aligned, the circuit operated with no detectable differential phase shift between the two amplifiers, frequency shift, or gain mismatch over a period of four months with large changes in ambient temperature and humidity.

3.5 Band-Block Filter

A study of the expression (C-2a, Appendix C) shows that there are terms in $40t$ (80 cps) which must be filtered out of the voltages in order to obtain Equations (C-3a) and (C-3b). A twin-T filter having a null at the frequency, $\frac{40}{2\pi}$, was used for this purpose. The circuit diagram is shown in Fig. 12. Frequency response curves for the two stage band-pass amplifier operated in conjunction with the band-block filter are shown in Fig. 13c.

3.6 Deflection Amplifiers

Commercially available oscilloscopes do not, as a rule, have identical amplifiers for both horizontal and vertical channels. Since these were required for this system, a pair of matched deflection amplifiers were designed.

The circuit for these deflection amplifiers consists of a split-load phase inverter driving two R-C coupled amplifiers in push-pull as is shown in Fig. 14.

3.7 Miscellaneous Notes

The mathematical treatment of Appendices B and C requires that both channels from the goniometer to output of this system be identical, both in phase and gain. For this reason all components were matched as closely as possible between channels.

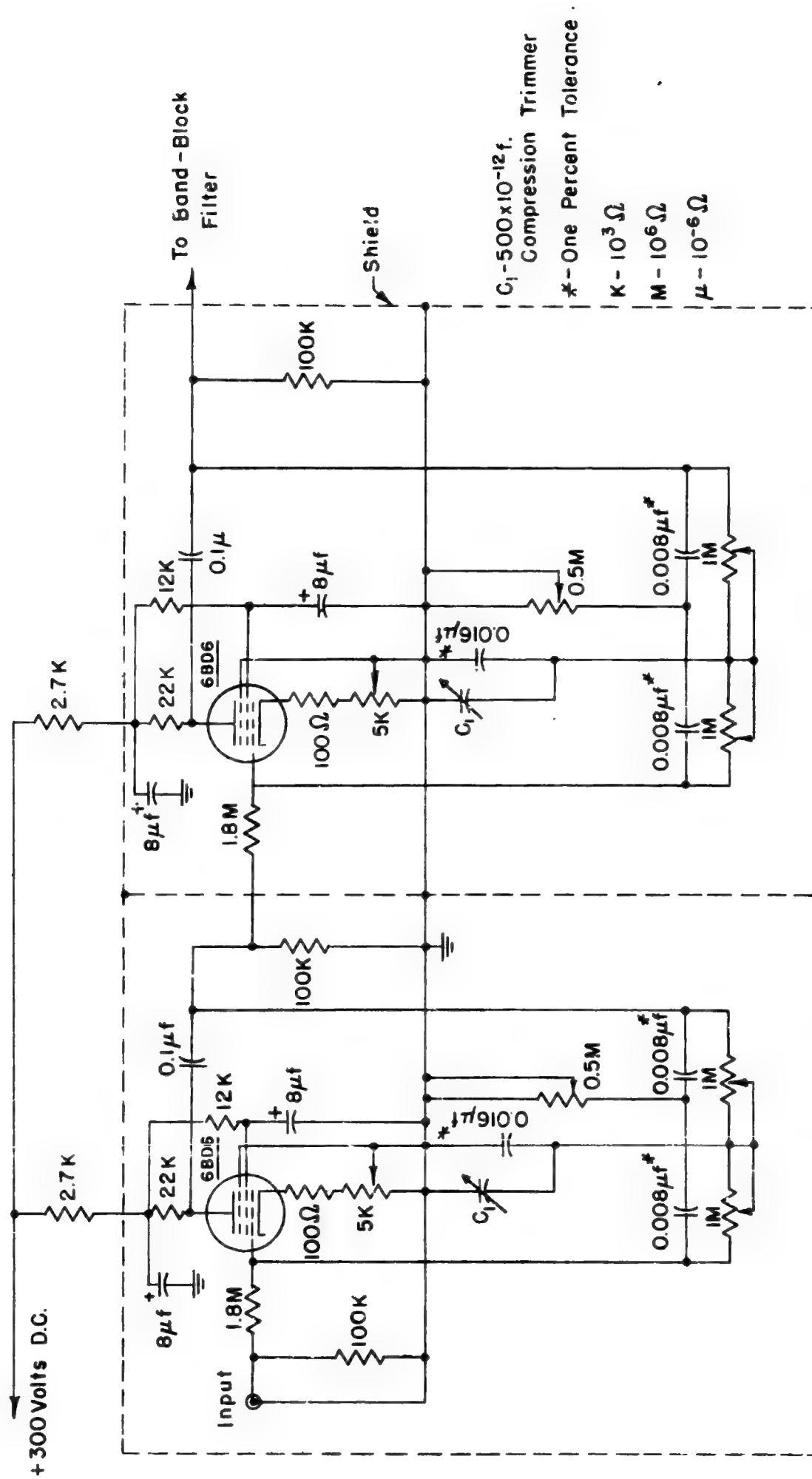
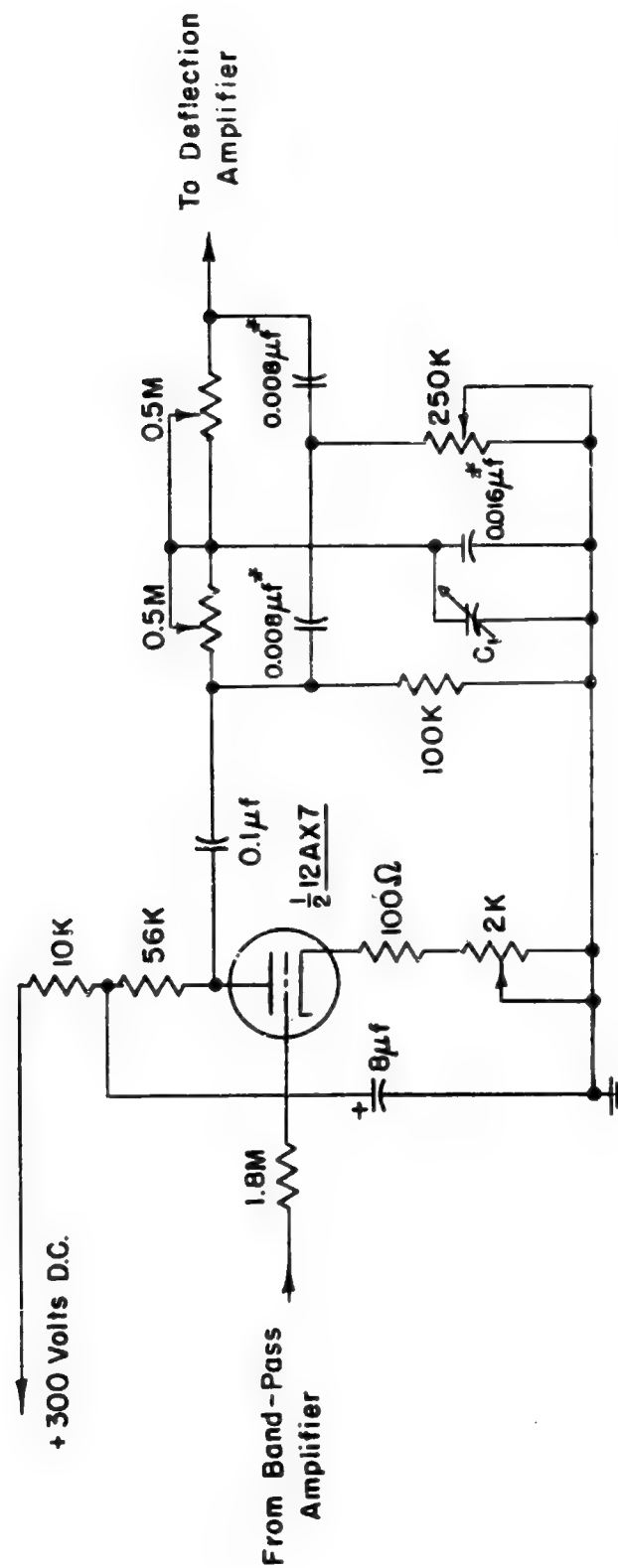


FIGURE 11 CIRCUIT DIAGRAM OF THE BAND-PASS AMPLIFIER



$C_1 = 500 \times 10^{12} \text{ f.}$

- One Percent Tolerance

K - $10^3 \Omega$

M - $10^6 \Omega$

μ - $10^{-6} \Omega$

FIGURE 12 CIRCUIT DIAGRAM OF THE BAND-BLOCK FILTER

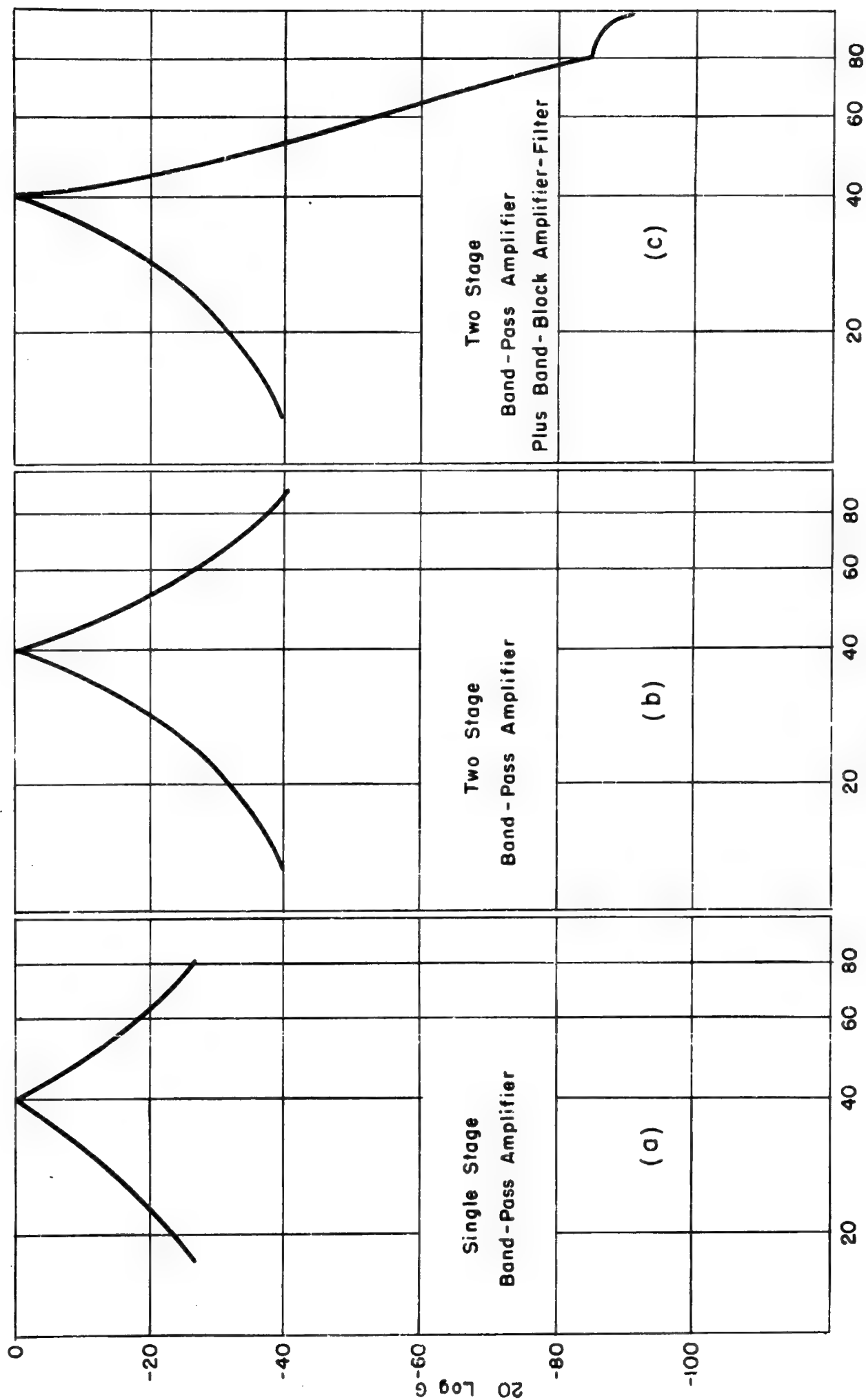


FIGURE 13 FREQUENCY RESPONSE CURVES OF BAND-PASS AMPLIFIER AND BAND-BLOCK FILTER

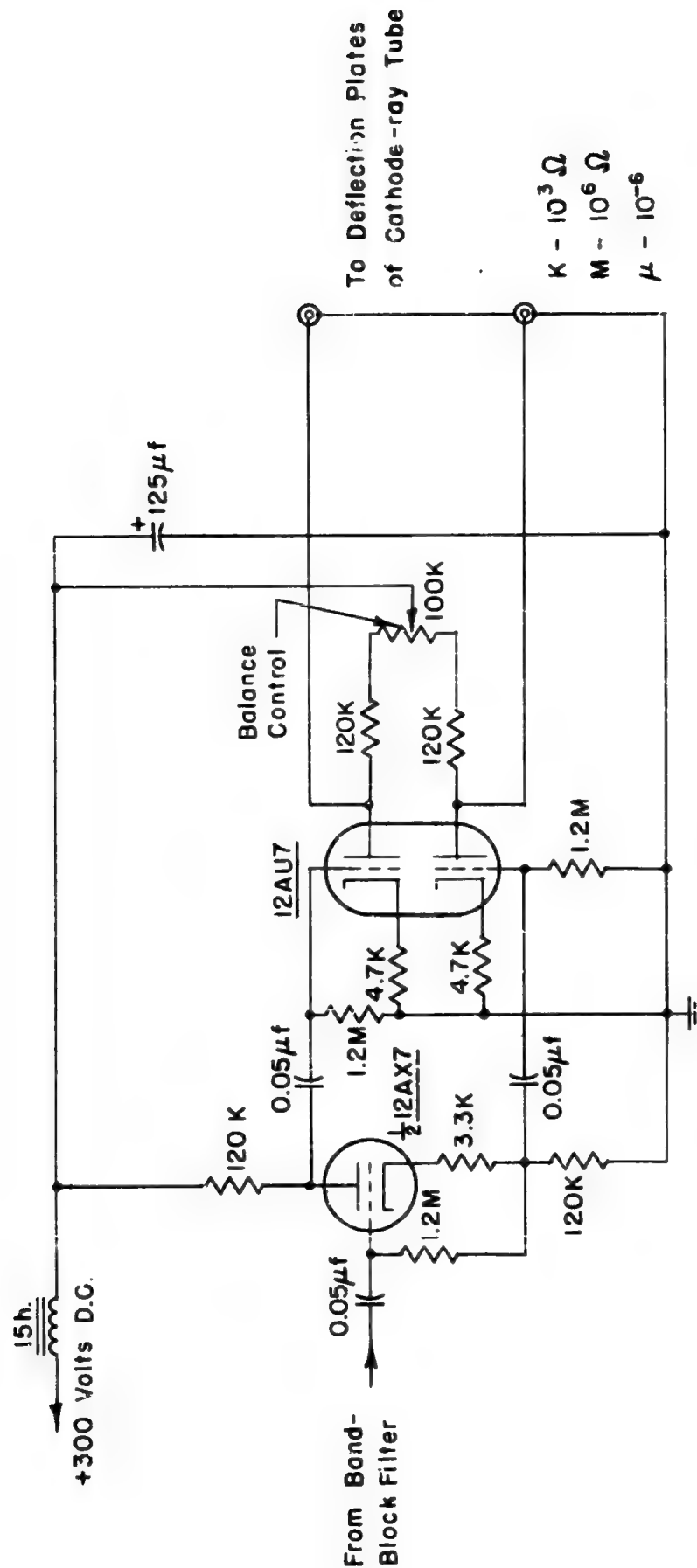


FIGURE 14 CIRCUIT DIAGRAM OF THE DEFLECTION AMPLIFIER

Low time constants were used in all coupling networks to insure minimum phase shift at the low frequency used. The frequency of operation of the system is determined by the rotation rate of the goniometer, which was in this case twelve hundred revolutions per minute, giving forty cycles per second as the center frequency of the band-pass amplifiers. This frequency could be changed by changing the rotation rate of the goniometers, or by performing the synchronous modulation by electronic means.

Most stages used a large amount of cathode degeneration to insure stable operation.

Each stage was individually decoupled from the B+ line to eliminate any cross-coupling or motor-boating..

4. EXPERIMENTAL RESULTS

Photographs of cathode-ray tube displays using this transformation system are shown in Figs. 15 and 16 with the modified ABI display, or "figure-eight" display. The bearing angle is read along the major axis of the ellipse in the transformed display and through the minimum of the modified display.

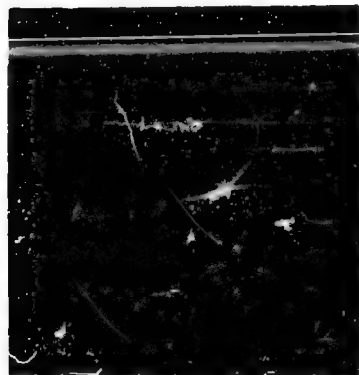
Figure 15 shows the displays for several cases of single frequency reception. The desired straight lines were obtained for only one received signal, and ellipses in the case of two signals of different bearing.

Since one complete pattern is obtained for each half revolution of the goniometer, any variation in the cosine coupling law for the goniometer can be seen as multiple traces in the transformed display. This effect is noticed particularly for the elliptical displays of Fig. 15. Slight nonlinearities in the multipliers are also noted as distortion of the elliptical patterns.

Figure 16 shows several displays obtained when two signals are received at different frequencies. The parallelogram displays contain all of the information of the Watson-Watt display except that this display is at a frequency of forty cycles per second and thus a longer time is required to obtain the complete display than would be required at the usual receiver IF. The interpretation is the same for both the Watson-Watt and the transformed display.

Non-linearities in the multipliers are particularly noticeable in the first picture of Fig. 16. In this case the received signal was approximately ten times the magnitude that it was in the other pictures in this figure, and the multiplier tubes were operating out of their linear range. Again, goniometer irregularities can be noticed as asymmetries in the displays, and lack of phase match between the two channels is noticed in the form of ellipsing of the display.

Bearing error, found by using a calibrated goniometer as the signal source, was less than three degrees if the signal strength was low enough to keep the multipliers operating in the linear region of their characteristics. The tubes were matched in the linear range and the mismatch occurring in the nonlinear range causes bearing error to increase. The bearing error figures could be improved by more careful matching of the two channels throughout the entire system.



a

Single Components



b



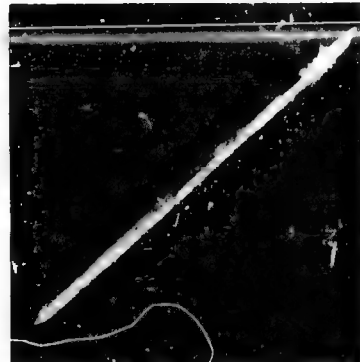
c

Two Signal Components



d

ABI FIGURE-EIGHT COMPONENT DISPLAYS

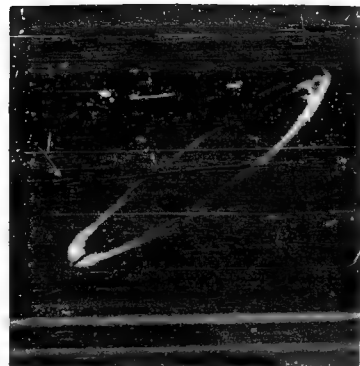


e

Single Components



f



g

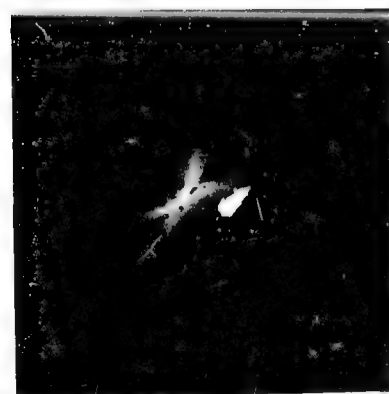
Two Signal Components



h

TRANSFORMED DISPLAYS

FIGURE 15 ABI "FIGURE-EIGHT" AND TRANSFORMED DISPLAYS FOR SIGNALS ON ONE FREQUENCY



a



b



c

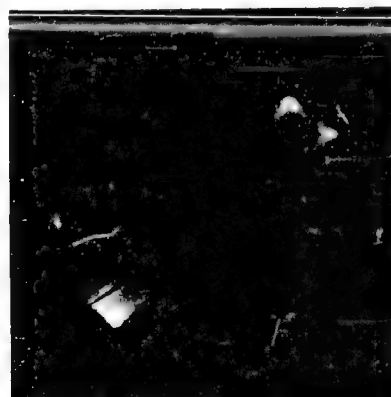


d

Neither Signal Component Modulated

One Component Modulated

ABI FIGURE-EIGHT COMPONENT DISPLAYS



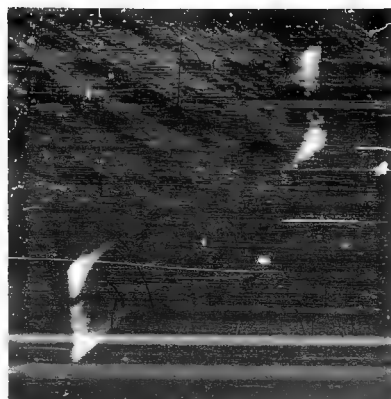
e



f

Neither Signal Component Modulated

One Component Modulated



g



h

FIGURE 16 ABI "FIGURE-EIGHT" AND TRANSFORMED DISPLAYS FOR SIGNALS ON TWO FREQUENCIES

While the extremely narrow pass-band of the amplifiers used eliminates nearly all of the modulation present on a signal, modulation frequencies that fall within the pass-band of the system can cause bearing errors. The last picture in Fig. 16 demonstrates this fact. In this case one of the received signals was modulated at a sixty cycle per second rate, with a modulation percentage of twenty. It can be seen that it is difficult to separate the bearings in this case. Modulation frequencies of over 160 cycles per second have no discernable effect on the bearing.

5. LIMITATIONS AND ALTERNATE METHODS OF OPERATION

This transformation system is limited by the non-linearities of the mixer tubes, the departures from the cosine coupling law in the goniometers, the requirement of matched channels from the ABI receiver to the output, and the requirement that all modulation of the signal components be of higher frequency than 160 cps.

The matching of channels is not a serious limitation for this fixed low frequency band, because at low frequencies such channels can be made rather insensitive to changes in tube constants and changes in temperature.

The system requires very sharp tuning for the very narrow output bandwidth of about 20 cps. To overcome this difficulty an automatic frequency control should be used on the variable tuned local oscillator. This, in combination with a crystal-controlled injection oscillator, would make the tuning much less critical.

Although the system described makes use of goniometers for performing the quadrature modulation and detection wherein the goniometers are driven by a motor at a rate $\theta/2\pi$, modulation using electron tubes could be used just as well, with $\theta/2\pi$ being supplied by an electronic oscillator. It may be noted in the development in Appendix C that undesired terms at the frequency $4 \theta/2\pi$ must be filtered out.

The development in Appendix D illustrates how modulation may introduce error, and how a system may be designed to reduce the error. If $2\theta < \sigma_{min}$ such that $\sigma_{min} \geq 8\theta$, the modulation will introduce no error. For the system described, the value of $\sigma_{min}/2\pi$ is 160 cps by this criterion, but it may be made considerably lower and not introduce appreciable bearing error.

Appendix D also shows that 2θ may be made quite high by making a proper choice with regard to the highest modulation frequency. The use of the high frequency is desirable for the case wherein bearings on flash transmissions are required. The output display is then "written" several times while the transmission is on, while for the low frequency case the display may be "written" only once or twice.

A word of warning is in order on this point. Because of the quadrature modulation at the input, the side bands must be equal in magni-

tude at the point of quadrature detection with $E_m \cos \theta t$ and $E_m \sin \theta t$. This places a limitation on a system in which 2θ is greater than σ_{\max} , but does not seriously affect the system for which 2θ is less than σ_{\min} , since in the latter case the side bands are close together, and the probability that they are different in magnitude by an appreciable amount is quite low.

It should be pointed out that the method of transforming the IF output of the ABI to the Watson-Watt display described in Section 2 may also be accomplished as follows:

First: perform operation B, i.e., linear modulation of the IF output with $E_n \cos (\omega t + 2\theta t)$, and filter out all terms containing ωt and $2\omega t$.

Second: quadrature modulate the above output with $E_m \cos \theta t$ and $E_m \sin \theta t$.

Third: filter out terms containing $4\theta t$ and DC terms.

Fourth: supply the resulting voltages to the deflection plates of the CRT as before.

This procedure gives the same result as is indicated by Eq. (4), and provides a somewhat simplified system in that the modulation by $E_n \cos (\omega t + 2\theta t)$ need be done in only one channel. The quadrature detection was done first in the system described because the goniometers used were designed to operate at radio frequencies.

6. CONCLUSIONS

A system has been described which transforms the IF output of the ABI receiver to a form which will produce a Watson-Watt type display. The system may be used in three ways: 1) to change the display of an existing ABI direction finder so that it may be used as a Watson-Watt type radio direction finder; 2) to give a Watson-Watt type display to be used as an auxiliary device with an ABI system; 3) to change the displays of each of several ABI systems to the Watson-Watt type, so that the resulting displays from a space distribution of such systems can be combined optically to form a composite display that can be readily interpreted. The third of these is believed to be the most important because of the potential use in obtaining accurate bearings on flash transmissions.

The goniometer method described here provided an excellent means for synchronizing the quadrature detection with the quadrature modulation, which is a necessity for a reliable system. The quadrature modulation and detection could be done electronically at much higher frequencies if the precautions outlined are followed.

Although the experiment was performed by operating on the output from a 175 kc amplifier, there is at present no apparent reason why the system could not be made to work with a complete ABI system.

The system is limited by the matching requirements of two channels, but this does not appear serious when the techniques for matching fixed frequency channels are considered. Another limitation appears when the incoming signal is modulated. By a proper choice of output frequency the limitations due to modulation may be minimized.

It has been shown that a bread-board model of the system described does give the predicted results.

It should be pointed out that it might be possible to achieve the desired result by some simpler method. In either case considerable developmental work would be necessary before a model of a transformation device is ready for field operation.

7. BIBLIOGRAPHY

1. Keen, R., *Wireless Direction Finding*, Iliffe and Sons, London, 1947, pp. 870-874.
2. Annis, Brunner, Campbell, Johnk, O'Meara, and Royal, *Technical Report No. 10*, University of Illinois, Direction Finding Research Laboratory, 1950, pp. 5-8.
3. de Walden, S. and Swallow, J.C., "The Relative Merits of Presentation of Bearings by Aural-Null and Twin-Channel Cathode-Ray Direction-Finders", *Journal of the Institute of Electrical Engineers*, Part III, Vol. 96, No. 42, July 1949, p. 307.
4. Costas, J.P., "Synchronous Detection of Amplitude Modulated Signals", *Proceedings of the National Electronics Conference*, Vol. 7, 1951, p. 121.
5. Everitt, W.L., *Communication Engineering*, McGraw-Hill Book Company, 1937, New York, p. 392.
6. Chance, Hughes, McNichol, Sayre, and Williams, *Waveforms*, McGraw-Hill Book Company, 1949, New York, p. 669.
7. Scott, I.H., "A New Type of Selective Circuit and Some Applications", *Proceedings of the Institute of Radio Engineers*, Vol. 26, Feb. 1938, p. 226.

APPENDIX A
EQUALITY OF ELLIPSING IN THE WATSON-WATT AND BLURRING
IN THE MODIFIED ABI

The expression for the Watson-Watt display in Fig. 17 is given by:

$$Z_{WW} = A \left[\cos \omega t e^{j\alpha} + \sum_{p=0}^N H_p \cos (\omega t + \phi_p) e^{j(\alpha + \beta_p)} \right] \quad (A-1)$$

The ABI "figure-eight" display at intermediate-frequency, hereafter called the modified ABI display, is given by:

$$Z_{ABI} = B \left[\cos \omega t \cos (\alpha - \theta t) e^{j\theta t} + \sum_{p=0}^N H_p \cos (\omega t + \phi_p) \cos (\alpha + \beta_p - \theta t) e^{j\theta t} \right] \quad (A-2)$$

For any particular goniometer displacement angle $(\theta t/2\pi)$ in Fig. 17 the magnitude of the radius vector in the modified ABI display is given by:

$$R_{ABI} = B \left[\cos \omega t \cos (\alpha - \theta t) + \sum_{p=0}^N \cos (\omega t + \phi_p) \cos (\alpha + \beta_p - \theta t) \right] \quad (A-3)$$

The project of the Watson-Watt display on a line at the angle $(\theta t/2\pi)$ is given in vector notation by the dot product:

$$C_Z = \vec{Z}_{WW} \cdot \left\{ \vec{i} \cos \theta t + \vec{j} \sin \theta t \right\}, \quad (A-4)$$

where \vec{i} and \vec{j} are unit vectors.

Then:

$$C_Z = A \left[\cos \omega t \cos (\alpha - \theta t) + \sum_{p=0}^N H_p \cos (\omega t + \phi_p) \cos (\alpha + \beta_p - \theta t) \right] \quad (A-5)$$

Comparing R_{ABI} to C_Z , it can be seen that:

$$C_Z = R_{ABI} \cdot \frac{A}{B} \quad (A-6)$$

From this it can be seen that the bearing angle, α , is the same in both cases, since C_Z is maximum when $\theta t/2\pi = \alpha$, and R_{ABI} is a minimum when $\theta t/2\pi = \alpha + \pi/2$. Then the angle read at the major axis of the ellipse on the Watson-Watt display is the same angle that is read at the minimum of the modified ABI display, or the maximum if the scale is shifted as in Fig. 17.

The "ellipticity" of the Watson-Watt display in Fig. 17 is defined as the ratio of the minor to the major axis, or:

$$\epsilon_{WW} = \left(\frac{\overline{CD}}{\overline{AB}} \right)_{WW} \quad (A-7)$$

The "blurring" of the ABI display is given by the ratio:

$$\epsilon_{ABI} = \left(\frac{\overline{CD}}{\overline{AB}} \right)_{ABI} \quad (A-8)$$

The minor axis of the ellipse is found by setting (θt) in Eq. (A-4) equal to $(\alpha + \pi/2)$. Then:

$$\overline{CD}_{WW} = A \sum_{p=0}^N H_p \cos(\omega t + \phi_p) \sin \beta_p \quad (A-9)$$

Similarly \overline{CD}_{ABI} is found by setting θt equal to $(\alpha + \pi/2)$ in Eq. (A-3).

Then:

$$\overline{CD}_{ABI} = B \sum_{p=0}^N H_p \cos(\omega t + \phi_p) \sin \beta_p \quad (A-10)$$

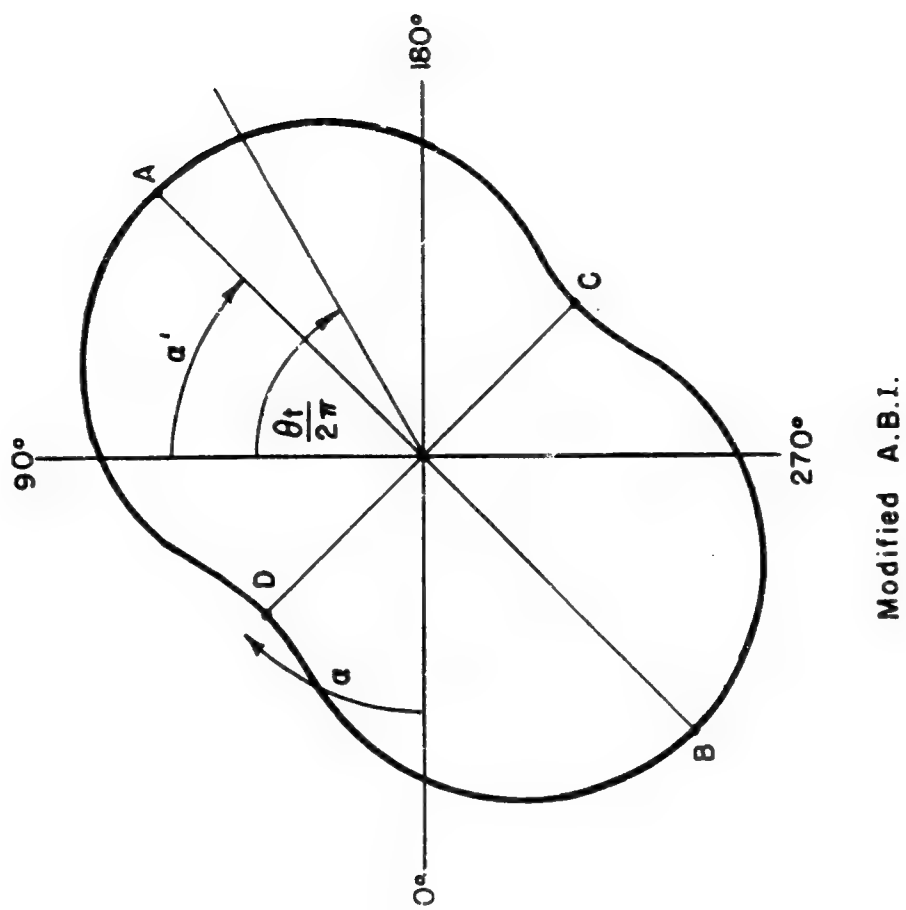
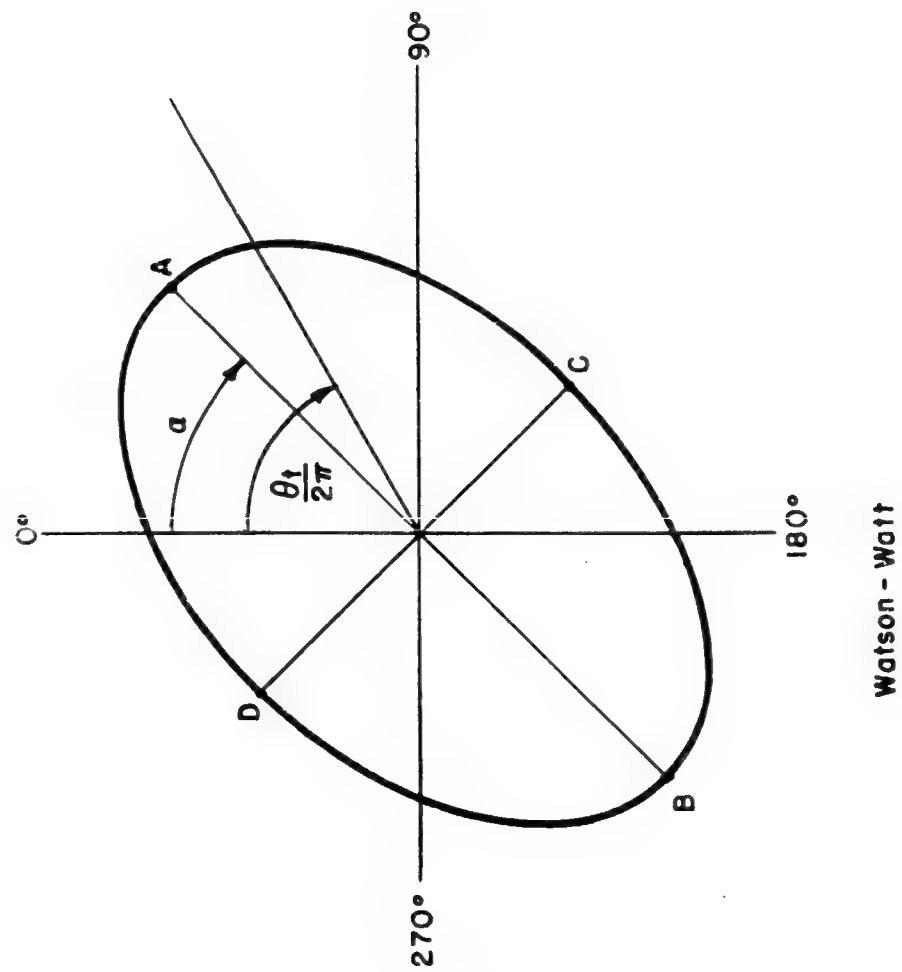


FIGURE 17 RELATIONSHIP BETWEEN ABI & WATSON-WATT DISPLAY

Similarly, for the major axis of the ellipse, let θt equal α in Eq. (A-4). Then:

$$\overline{AB}_{WW} = A \left[\cos \omega t + \sum_{p=0}^N H_p \cos (\omega t + \phi_p) \cos \beta_p \right] \quad (A-11)$$

The length \overline{AB}_{ABI} is found by setting θt equal to α in Eq. (A-3).

Then:

$$\overline{AB}_{ABI} = B \left[\cos \omega t + \sum_{p=0}^N H_p \cos (\omega t + \phi_p) \cos \beta_p \right] \quad (A-12)$$

It can be seen that:

$$\frac{\overline{CD}_{WW}}{\overline{AB}_{WW}} = \frac{\overline{CD}_{ABI}}{\overline{AB}_{ABI}} \quad (A-13)$$

and

$$\epsilon_{WW} = \epsilon_{ABI} \quad (A-14)$$

APPENDIX B

DEVELOPMENT OF THE DISPLAY EQUATION FOR THE TRANSFORMATION
METHOD USING SQUARE-LAW BALANCED MODULATORS

If the ABI IF output:

$$E = A \cos \omega t \cos (\alpha - \theta t) + A \sum_{p=0}^N H_p \cos (\omega t + \phi_p) \cos (\alpha + \beta_p - \theta t) \quad (B-1)$$

is applied to the search coil of a second goniometer with the same rotation rate and displacement angle as the receiver goniometer, the resulting output voltages are given by:

$$E_1 = \frac{B}{2} \left[\cos (\omega t) \{ \cos \alpha + \cos (\alpha - 2\theta t) \} + \sum_{p=0}^N H_p \cos (\omega t + \phi_p) \{ \cos (\alpha + \beta_p) + \cos (\alpha + \beta_p - 2\theta t) \} \right] \quad (B-2a)$$

$$E_2 = \frac{B}{2} \left[\cos (\omega t) \{ \sin \alpha - \sin (\alpha - 2\theta t) \} + \sum_{p=0}^N H_p \cos (\omega t + \phi_p) \{ \sin (\alpha + \beta_p) - \sin (\alpha + \beta_p - 2\theta t) \} \right] \quad (B-2b)$$

This accomplishes the quadrature detection with $E_m \cos \theta t$ and $E_m \sin \theta t$ components.

Modulating these voltages with $E_n \cos (\omega t + \gamma)$ in square-law balanced modulators gives

$$E_1' = C_1 \left[\{ \cos (2\omega t + \gamma) + \cos \gamma \} \{ \cos \alpha + \cos (\alpha - 2\theta t) \} + \sum_{p=0}^N H_p \{ \cos (2\omega t + \gamma + \phi_p) + \cos (\gamma - \phi_p) \} \{ \cos (\alpha + \beta_p) + \cos (\alpha + \beta_p - 2\theta t) \} \right] \quad (B-3a)$$

$$E_2' = C_1 \left[\begin{aligned} &\{\cos (2\omega t + \gamma) + \cos \gamma\} \{\sin \alpha - \sin (\alpha - 2\theta t)\} \\ &+ \sum_{p=0}^N H_p \{\cos (2\omega t + \gamma + \phi_p) + \cos (\gamma - \phi_p)\} \{\sin (\alpha + \beta_p) \\ &\quad - \sin (\alpha + \beta_p - 2\theta t)\} \end{aligned} \right] \quad (B-3b)$$

If γ were held constant and all AC terms filtered out, these voltages would take the forms:

$$E_1'' = C_2 \cos \gamma \cos \alpha + C_2 \sum_{p=0}^N H_p \cos (\gamma - \phi_p) \cos (\alpha + \beta_p) \quad (B-4a)$$

$$E_2'' = C_2 \cos \gamma \sin \alpha + C_2 \sum_{p=0}^N H_p \cos (\gamma - \phi_p) \sin (\alpha + \beta_p) \quad (B-4b)$$

Applying these voltages to a pair of gating circuits with the characteristics:

$$E_{out} = C_3 E_a E_b' = C_3 E_a \sin \rho t \quad (B-5)$$

where E_a is one of the DC voltages, E_1'' or E_2'' and ρ is any convenient value, then:

$$E_1'' = D \cos \gamma \cos \alpha \sin \rho t + D \sum_{p=0}^N H_p \cos (\gamma - \phi_p) \cos (\alpha + \beta_p) \sin \rho t \quad (B-6a)$$

$$E_2'' = D \cos \gamma \sin \alpha \sin \rho t + D \sum_{p=0}^N H_p \cos (\gamma - \phi_p) \sin (\alpha + \beta_p) \sin \rho t \quad (B-6b)$$

The display obtained by applying these voltages to the orthogonal plates of a CRT may be represented by:

$$Z = K \sin \rho t \left[\cos \gamma e^{j\alpha} + \sum_{p=0}^N H_p \cos (\gamma - \phi_p) e^{j(\alpha + \beta_p)} \right] \quad (B-7)$$

This is the same as Eq. (3).

APPENDIX C DEVELOPMENT OF THE DISPLAY EQUATION FOR THE TRANSFORMATION METHOD USING LINEAR MIXERS

An alternate method of transforming the ABI IF output to the Watson-Watt display is to apply the voltages of Eq. (B-2), Appendix B, to linear mixers which have the characteristics:

$$E_{out} = FE_a + GE_b + HE_a E_b \quad (C-1)$$

where E_a is E_1 or E_2 and $E_b = E_m \cos (\omega t + 2\theta t)$.

The resulting voltages are given by:

$$\begin{aligned} E_1' = & \frac{FB}{2} \left[\cos \omega t \{ \cos \alpha + \cos (\alpha - 2\theta t) \} \right. \\ & + \sum_{p=0}^N H_p \cos (\omega t + \phi_p) \{ \cos (\alpha + \beta_p) + \cos (\alpha + \beta_p - 2\theta t) \} \left. \right] + GE_m \cos (\omega t + 2\theta t) \\ & + E_m \frac{HB}{4} \left[\cos (\alpha) \{ \cos (2\omega t + 2\theta t) + \cos 2\theta t \} + \cos (\alpha - 2\theta t) \cos (2\omega t + 2\theta t) \right. \\ & + \frac{1}{2} \cos \alpha + \frac{1}{2} \cos (\alpha - 4\theta t) \\ & + \sum_{p=0}^N H_p \left\{ \{ \cos (2\omega t + 2\theta t + \phi_p) \} \{ \cos (\alpha + \beta_p) + \cos (\alpha + \beta_p - 2\theta t) \} \right. \\ & + \cos (2\theta t - \phi_p) \cos (\alpha + \beta_p) + \frac{1}{2} \cos (\alpha + \beta_p - \phi_p) \\ & \left. \left. + \frac{1}{2} \cos (\alpha + \beta_p - 4\theta t - \phi_p) \right\} \right] \quad (C-2a) \end{aligned}$$

The equation for E_2' is similar and will contain terms at the same frequencies as the equation for E_1' .

Filtering these two voltages to eliminate DC terms and terms containing ωt , $2\omega t$, and $4\omega t$ gives:

$$E_1'' = K \left[\cos \alpha \cos 2\theta t + \sum_{p=0}^N H_p \cos (\alpha + \beta_p) \cos (2\theta t - \phi_p) \right] \quad (C-3a)$$

$$E_2'' = K \left[\sin \alpha \cos 2\theta t + \sum_{p=0}^N H_p \sin (\alpha + \beta_p) \cos (2\theta t - \phi_p) \right] \quad (C-3b)$$

The display obtained by applying these voltages to the orthogonal plates of a CRT may be represented by:

$$Z = M \left[\cos 2\theta t e^{j\alpha} + \sum_{p=0}^N H_p \cos (2\theta t - \phi_p) e^{j(\alpha + \beta_p)} \right] \quad (C-4)$$

which is the same as Eq. (4).

APPENDIX D

THE EFFECT OF MODULATION ON THE TRANSFORMATION SYSTEM

In the incoming signal is a modulated signal which may be represented by $E_s \cos \omega t (1 + \sum_{q=1}^S m_q \cos \sigma_q t)$, Eq. (B-2a) becomes:

$$E_1 = \frac{B}{2} \left[\cos \omega t (1 + \sum_{q=1}^S m_q \cos \sigma_q t) \{ \cos \alpha + \cos (\alpha - 2\theta t) \} \right. \\ \left. + \sum_{p=0}^N H_p \cos (\omega t + \phi_p) (1 + \sum_{q=1}^S m_q \cos \sigma_q t) \{ \cos (\alpha + \beta_p) + \cos (\alpha + \beta_p - 2\theta t) \} \right].$$

(D-1a)

After quadrature modulation with $\cos \theta t$ and $\sin \theta t$, and after modulation with $E_b = E_m \cos (\omega t + 2\theta t)$, by the method shown in Appendix C, and after filtering out terms containing ωt and $2\omega t$, the above equation becomes:

$$E_1^* = \frac{E_m IB}{4} \left[\cos 2\theta t (1 + \sum_{q=1}^S m_q \cos \sigma_q t) \{ \cos \alpha + \cos (\alpha + 2\theta t) \} \right. \\ \left. + \sum_{p=0}^N H_p \cos (2\theta t - \phi_p) (1 + \sum_{q=1}^S m_q \cos \sigma_q t) \{ \cos (\alpha + \beta_p) \right. \\ \left. + \cos (\alpha + \beta_p - 2\theta t) \} \right],$$

(D-2a)

which may be written as follows:

$$E_1^* = \frac{E_m IB}{4} \left[\cos 2\theta t \{ \cos \alpha + \cos (\alpha - 2\theta t) \} + \sum_{p=0}^N H_p \cos (2\theta t - \phi_p) \{ \cos (\alpha + \beta_p) \right. \\ \left. + \cos (\alpha + \beta_p - 2\theta t) \} \right]$$

(D-3a)

$$\begin{aligned}
& + \sum_{q=1}^S m_q \cos \sigma_q t \cos 2\theta t \{ \cos \alpha + \cos (\alpha - 2\theta t) \} \\
& + \sum_{q=1}^S m_q \cos \sigma_q t \sum_{p=0}^N H_p \cos (2\theta t - \phi_p) \cdot \{ \cos (\alpha + \beta_p) + \cos (\alpha + \beta_p - 2\theta t) \} \quad]
\end{aligned}$$

(D-3a cont'd)

This equation may be expanded into:

$$\begin{aligned}
E_1^* = \frac{E_{mHB}}{4} & \left[\cos \alpha \cdot \cos 2\theta t + \frac{1}{2} \cos \alpha + \frac{1}{2} \cos (\alpha - 4\theta t) \right. \\
& + \sum_{p=0}^N H_p \{ \cos (\alpha + \beta_p) \cos (2\theta t - \phi_p) + \frac{1}{2} \cos (\alpha + \beta_p - \phi_p) \\
& \qquad \qquad \qquad + \frac{1}{2} \cos (\alpha + \beta_p + \phi_p - 4\theta t) \} \\
& + \sum_{q=1}^S \frac{m_q}{2} \{ \cos \alpha [\cos (2\theta t + \sigma_q t) + \cos (2\theta t - \sigma_q t)] \\
& \qquad \qquad \qquad + \frac{1}{2} \cos (\sigma_q t + \alpha) + \frac{1}{2} \cos (\alpha - 4\theta t - \sigma_q t) \} \\
& + \sum_{q=1}^S \sum_{p=0}^N m_q H_p \{ \cos (\alpha + \beta_p) [\cos (2\theta t + \sigma_q t - \phi_p) + \cos (2\theta t - \sigma_q t - \phi_p)] \\
& \qquad \qquad \qquad + \frac{1}{2} \cos (\alpha + \beta_p + \sigma_q t - \phi_p) + \frac{1}{2} \cos (4\theta t + \sigma_q t - \phi_p - \alpha - \beta_p) \\
& \qquad \qquad \qquad + \frac{1}{2} \cos (\alpha + \beta_p - \sigma_q t - \phi_p) + \frac{1}{2} \cos (4\theta t - \sigma_q t - \phi_p - \alpha - \beta_p) \} \quad]
\end{aligned}$$

(D-4a)

The filters used eliminate $4\theta t$ and DC terms. It is safe to assume that all terms containing angular frequencies greater than 4θ may also be filtered out. When this is done Eq. (D-4a) becomes:

$$\begin{aligned}
E_1^* = \frac{E_{HB}}{4} & \left[\cos \alpha \cos 2\theta t + \sum_{p=0}^N H_p \cos (\alpha + \beta_p) \cos (2\theta t - \phi_p) \right. \\
& + \sum_{q=1}^S \frac{m_q}{2} \{ \cos \alpha [\cos (2\theta t + \sigma_q t) + \cos (2\theta t - \sigma_q t)] \\
& + \frac{1}{2} \cos (\sigma_q t + \alpha) + \frac{1}{2} \cos (\sigma_q t - \alpha) + \frac{1}{2} \cos (4\theta t - \sigma_q t - \alpha) \} \\
& + \sum_{q=1}^S \sum_{p=0}^N \frac{m_q H_p}{2} \{ \cos (\alpha + \beta_p) [\cos (2\theta t + \sigma_q t - \phi_p) + \cos (2\theta t - \sigma_q t - \phi_p)] \\
& + \frac{1}{2} \cos (\alpha + \beta_p + \sigma_q t - \phi_p) + \frac{1}{2} \cos (\alpha + \beta_p - \sigma_q t - \phi_p) \\
& + \frac{1}{2} \cos (4\theta t - \sigma_q t - \phi_p - \alpha - \beta_p) \} \left. \right] \quad (D-5a)
\end{aligned}$$

The relation for E_2^* may be developed in a similar manner. It will contain terms at the same frequencies as those indicated in the expression for E_1^* .

The equation (D-5a) contains several undesired terms brought about by the modulation. These terms may be eliminated by a proper choice of $2\theta t$ with respect to the modulation frequencies $\sigma_q t/2\pi$. If $\sigma_{\min}/2\pi$ represents the lowest probable modulation frequency, and if $\sigma_{\min} = 8\theta$, all objectionable terms in Eq. (D-5a) will be eliminated if the filters reject all components above $4\theta t$. In the system described in this report $2\theta/2\pi$ is 40 cps, so that the lowest modulation component that will not cause trouble is 160 cps. Actually the bandpass amplifier used has good rejection at 60 cps, so that modulation components as low as 140 cps should cause no trouble; and since the effect of such components is diminished by the modulator constant and by the modulation index, modulation components even lower than 140 cps would ordinarily not introduce appreciable error. This will take care of most speech and code transmissions.

Another possibility that arises is to make $2\theta t$ above the modulation band. In this case the $(2\theta t \pm \sigma_q t)$ terms are not to be classified as

undesirable since they are the side bands due to modulation of 2θ by $\sigma_q t$. If $\sigma_{max}/2\pi$ represents the maximum modulation frequency, the bothersome terms contain $\sigma_q t$ alone and $(4\theta t - \sigma_q t)$. It would be necessary to choose $2\theta/2\pi$ above $\sigma_{max}/2\pi$, and make the band pass characteristic about $2\theta/2\pi$ sharp enough to eliminate the undesired terms. If, for example $\frac{\sigma_{max}}{2\pi} = 5$ kc, $2\theta/2\pi$ might be made 10 kc and the band pass

amplifiers at the output designed for 80 db rejection at ± 5 kc. The resulting output would then be such that the modulation would cause no error, provided that the side bands at the angular frequencies $(\omega \pm \theta)$ are equal in magnitude at the point of quadrature detection with $E_m \cos \theta t$ and $E_m \sin \theta t$.